Fatigue Fract. Engng Mater. Struct. Vol. 13, No. 3, pp. 297–310, 1990
Printed in Great Britain.

8756-758X/90 $3.00 + 0.00

EFFECT OF SPECIMEN GEOMETRY ON FATIGUE CRACK GROWTH IN PLANE STRAIN—II. OVERLOAD RESPONSE

H. R. SHERCLIFF and N. A. FLECK
Cambridge University Engineering Department, Trumpington Street, Cambridge CB2 1PZ, England

(*Received in final form* 23 *October* 1989)

Abstract—Overload tests were performed on compact tension (CT) and centre cracked panel (CCP) specimens made from 6082-T6 aluminium alloy and BS4360 50B structural steel. The specimens were sufficiently thick for plane strain conditions to apply. Consistently greater retardation was observed in the CCP geometry than in the CT geometry. The effect of geometry is understood in terms of the T-stress and its effect on the overload plastic zone size. This was confirmed by biaxial tests in which the T-stress was varied independently of K. The action of machining off the side faces of an overloaded specimen did not eliminate the retardation; thus overload retardation is not due to a propping open by the surface regions of the specimen. Discontinuous closure was observed after overloads in the aluminium alloy and steel, as predicted by finite element calculations.

NOMENCLATURE

a = crack length
A = material constant
D = delay ratio
E = Young's modulus
$K, (\Delta K)$ = stress intensity factor (range)
N = number of cycles
n = strain hardening exponent
P = load
R = R ratio (P_{min}/P_{max})
r_{ps} = surface plastic zone size
T = T-stress
v = displacement perpendicular to crack
W = specimen width (Bend), half-width (CCP)
x, x_0 = distance ahead of crack tip, and crack tip offset
ϵ_{yy} = true strain perpendicular to crack
ν = Poisson's ratio
σ_{res} = residual stress
σ_y = yield stress
σ_{yy} = normal stress perpendicular to crack
σ_1, σ_2 = normal and transverse applied stress, biaxial specimen

Subscripts
min = minimum
max = maximum
op = opening
ol = overload
ca = constant amplitude

INTRODUCTION

It is well known that overloads can retard crack growth over a subsequent increment of crack growth. Plasticity-induced crack closure may be a major mechanism causing this retardation. The

overload plastic zone acts as a wedge of residual stretched material as the crack advances through it, reducing ΔK_{eff}. This argument is generally accepted for plane stress conditions but not for plane strain.

Finite element calculations

The effect of an overload on plasticity-induced crack closure following a tensile overload was modelled using the finite element method. Using a program developed by Newman [1] and discussed elsewhere [2, 3], crack growth was simulated in centre-cracked panels (CCP) and in Bend specimens made from elastic-perfectly plastic material of yield strain 0.005 and Poisson's ratio $\nu = 0.3$.

The finite element mesh consisted of 1967 two-dimensional constant strain triangular elements; near the crack tip the elements were arranged to form a series of squares and their diagonals in order to accommodate incompressible flow [4]. Fictitious springs were used to change the boundary conditions associated with crack growth, crack closure or crack opening. Fatigue crack growth was simulated by release of the crack tip node at $K_{\max}$, followed by a single loading cycle: $K_{\max} \rightarrow K_{\min} \rightarrow K_{\max}$, and this process was then repeated. Typically, a crack was advanced by 6 small element sizes (each of size 0.00078125 W, where W is the width of the specimen) from an initial crack length a of 0.486719 W, under fatigue loading. An overload of range twice the baseline loading was applied with no crack growth, and then baseline loading was resumed for a crack growth increment of 30 element sizes. Both plane stress and plane strain conditions were considered; for the plane stress runs, the baseline $K_{\max} = 0.11\ \sigma_y \sqrt{W}$ and $K_{\min} = 0$, while for the plane strain runs, the baseline $K_{\max} = 0.22\ \sigma_y \sqrt{W}$ and $K_{\min} = 0$.

The overload plastic zones at $K = K_{ol}$ are shown in Fig. 1 for plane stress and for plane strain. The overload plastic zone extends further ahead of the crack tip under plane stress conditions than under plane strain conditions. While specimen geometry has little influence upon plastic zone shape in plane stress, the zone is larger and extends further ahead of the crack for the CCP geometry than for the Bend geometry under plane strain conditions. Larsson and Carlsson [5] have shown that this variation in plastic zone shape with specimen geometry for plane strain is due to the different magnitudes of the "T-stress" near the crack tip in the two geometries. Specifically, the non-singular second term in the series expansion of the normal stress parallel to the crack plane differs from one geometry to the next, and has a strong influence on plastic zone size and shape.

A plot of the ratio of crack opening load to the maximum load of the fatigue cycle, $P_{\text{op}}/P_{\max}$, is given in Fig. 2 as a function of crack extension from the overload location, for both geometries

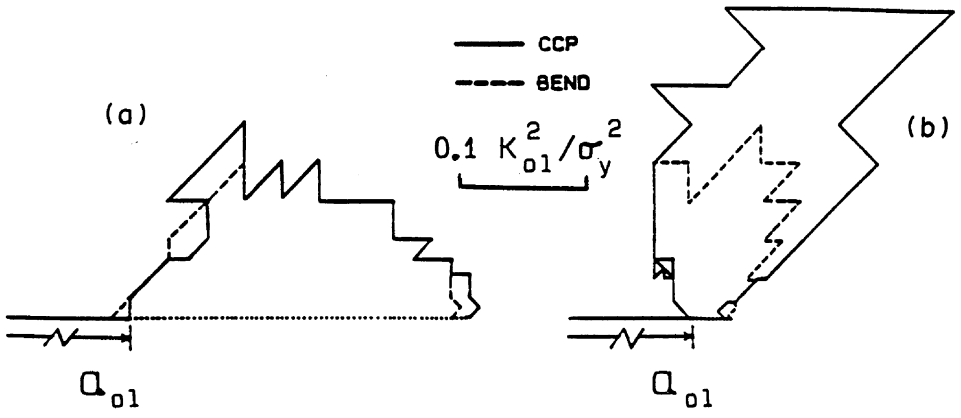

Fig. 1. Finite element predictions of overload plastic zones for: (a) plane stress; (b) plane strain.

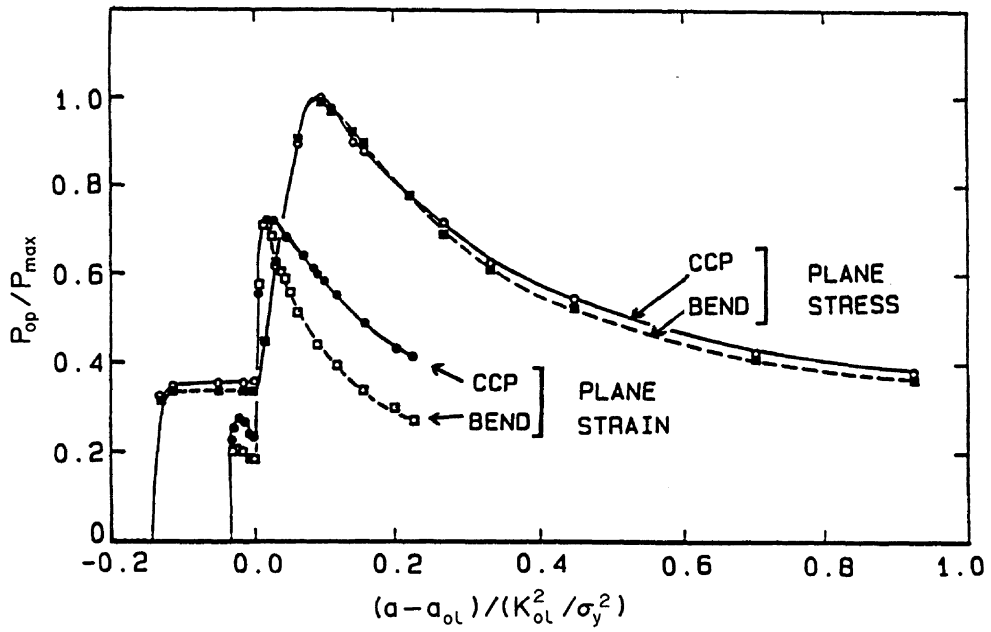

Fig. 2. Finite element prediction of crack opening response following an overload; overload ratio = 2 and $R = 0$.

and stress states. It is clear that the crack opening load is higher and persists over a larger crack growth increment for plane stress conditions than for plane strain. Under plane stress loading, specimen geometry has little influence on the closure transient, whereas under plane strain loading there is a stronger closure transient in the CCP geometry than the Bend geometry. This is consistent with the fact that the overload plastic zone is larger in the CCP geometry than in the Bend geometry, under plane strain conditions.

Now consider the crack opening response following an overload, see Fig. 3. In both plane stress and plane strain the crack opening profile at minimum load shows that closure occurs at a point remote from the crack tip once the crack has advanced some way beyond the overload locations. This phenomenon of "discontinuous closure" has been postulated from experimental studies in which the crack growth rate inferred from closure measurements falls below the true growth rate [6, 7]. In effect, fatigue damage can occur when the tip is open, which can be at loads below that at which the crack faces first touch.

In the present study, the influence of specimen geometry on retardation response is determined for plane strain conditions. The influence of surface layers on bulk response is addressed. Biaxial tests are reported where the load biaxiality during an overload is varied. Finally, a simple analytical model is presented to predict the plasticity-induced closure response following an overload.

OVERLOAD TESTS

Single overloads were applied to 10 mm and 16 mm thick specimens made from 6082-T6 aluminium alloy and BS4360 50B structural steel. Full details on these materials are given in Part I of this paper. Both compact tension (CT) and centre cracked panel (CCP) geometries were used.

Fatigue cracks were grown transverse to the roll direction at a constant stress intensity range ΔK and constant load ratio R ($= P_{min}/P_{max}$), by manually shedding the load with crack growth. The test frequency was 5 Hz. The crack length was monitored using a travelling microscope. Crack closure was monitored using back face strain and crack mouth displacement gauges. An offset

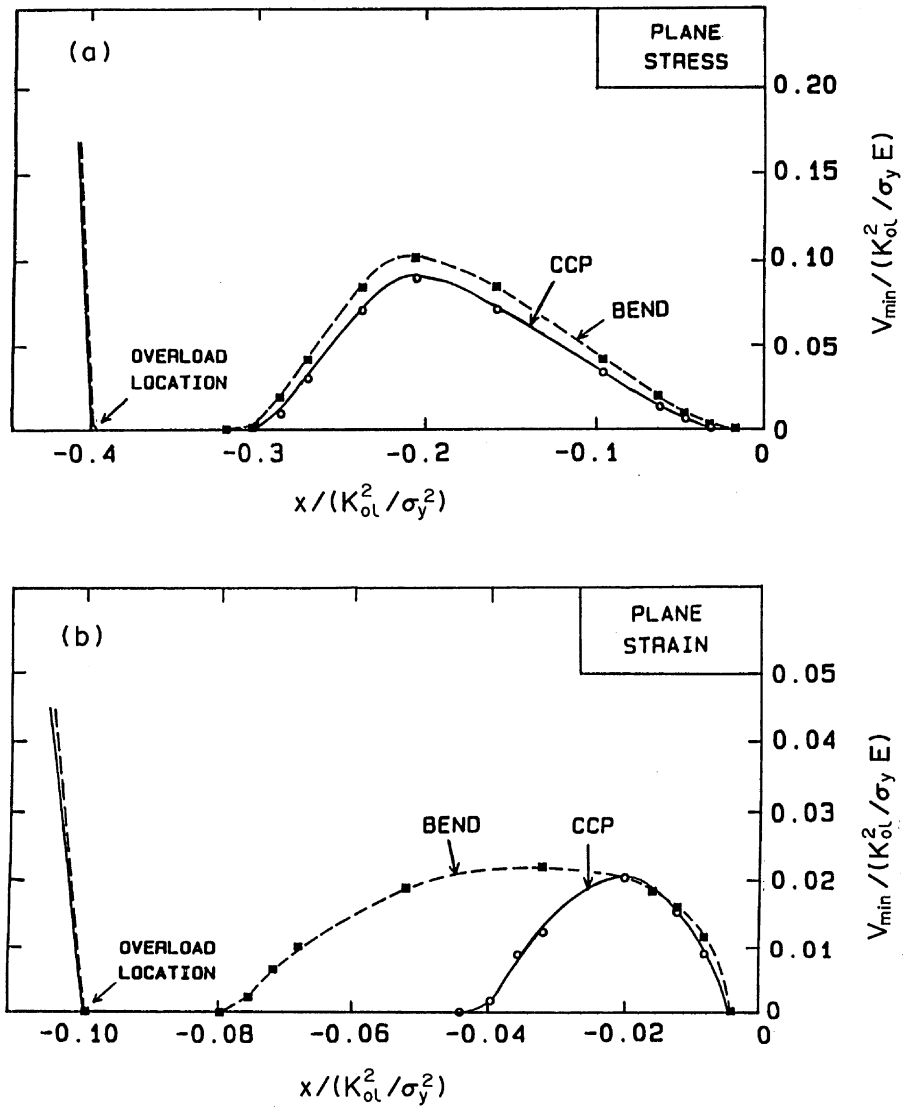

Fig. 3. Finite element predictions of crack opening profiles at K_{min} following an overload for: (a) plane stress, crack has advanced 0.4 $(K_{ol}/\sigma_y)^2$ ahead of the overload location; (b) plane strain, crack has advanced 0.1 $(K_{ol}/\sigma_y)^2$ ahead of the overload location.

procedure and low-pass filters were used to improve accuracy of the closure measurements. Further information about the instrumentation used is given in Refs [8, 9].

Single overloads were applied upon interruption of a test at constant baseline stress intensity range ΔK and load range, R. The range of the overload cycle ΔK_{ol} divided by ΔK (the "overload ratio") was varied from 1.5 to 2.0, and the baseline R ranged from 0.05 to 0.5.

The severity of the retardation was measured by a delay ratio D defined by

$$D = \frac{N_{ol}}{N_{ca}} \tag{1}$$

where N_{ca} is the number of cycles required at the pre-overload growth rate to grow the crack over the distance for which the growth rate is retarded, and N_{ol} is the number of additional cycles caused

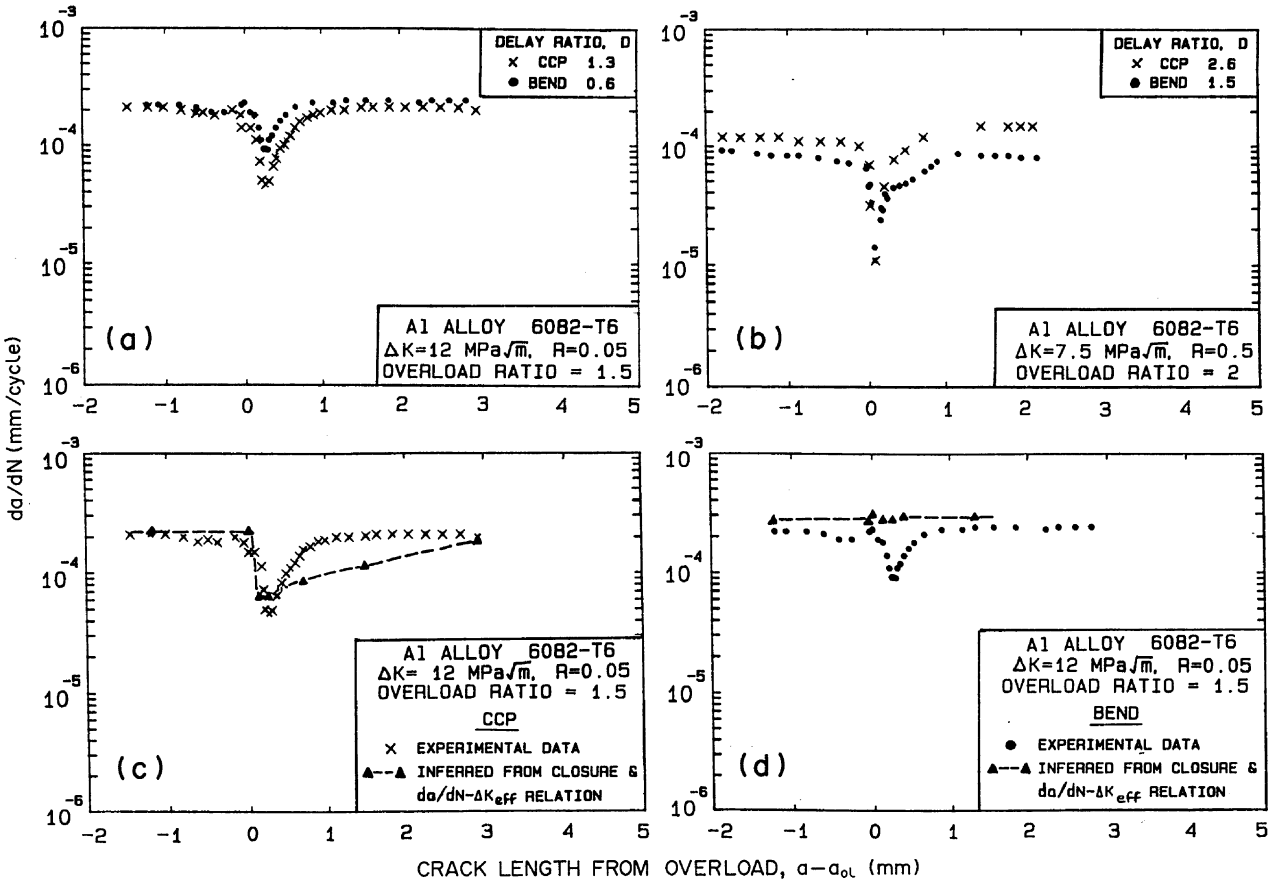

Fig. 4. Measured crack growth rates following a single overload for CCP and Bend geometries in Al alloy 6082-T6. (a) $K_{ol}/\sigma_y\sqrt{W} = 0.28$ (CCP and Bend). (b) $K_{ol}/\sigma_y\sqrt{W} = 0.34$ (CCP and Bend). (c) Measured and inferred growth rates (CCP). (d) Measured and inferred growth rates (Bend).

by the overload.* The delay ratio is therefore equal to zero if there is no retardation. The value of D is determined graphically from a plot of crack length vs number of cycles.

Results

To compare the geometries the da/dN transient is plotted against crack growth increment from the point of application of the overload, see Figs 4(a), 4(b) and 5(a).

The delay ratio is included in the figures, and the value of $K_{ol}/\sigma_y\sqrt{W}$ is given for comparison with the FEM value of 0.44. In all cases the retardation is more pronounced in the CCP geometry than in the Bend specimen, in terms of the crack increment over which the transient occurs and the delay ratio.

The retardation transients are compared with those inferred from closure measurements and the characteristic da/dN vs ΔK_{eff} relations, see Fig. 4(c, d) and 5(b, c). For the steel, the overload plastic zone size was sufficiently large to give a closed crack increment of sufficient magnitude to give reliable closure measurements. The inferred and measured growth rates show good agreement, except for the period when crack growth rates are recovering from the minimum value. In this regime, the crack is open near its tip and shut near the overload location at loads below the crack opening load. This phenomenon of discontinuous closure, giving rise to anomalously high crack opening loads has already been described by Fleck [7].

*Thus N_{ca} plus N_{ol} is the number of cycles between the end of steady state growth at the instant of overload to the re-commencement of steady state growth following the overload.

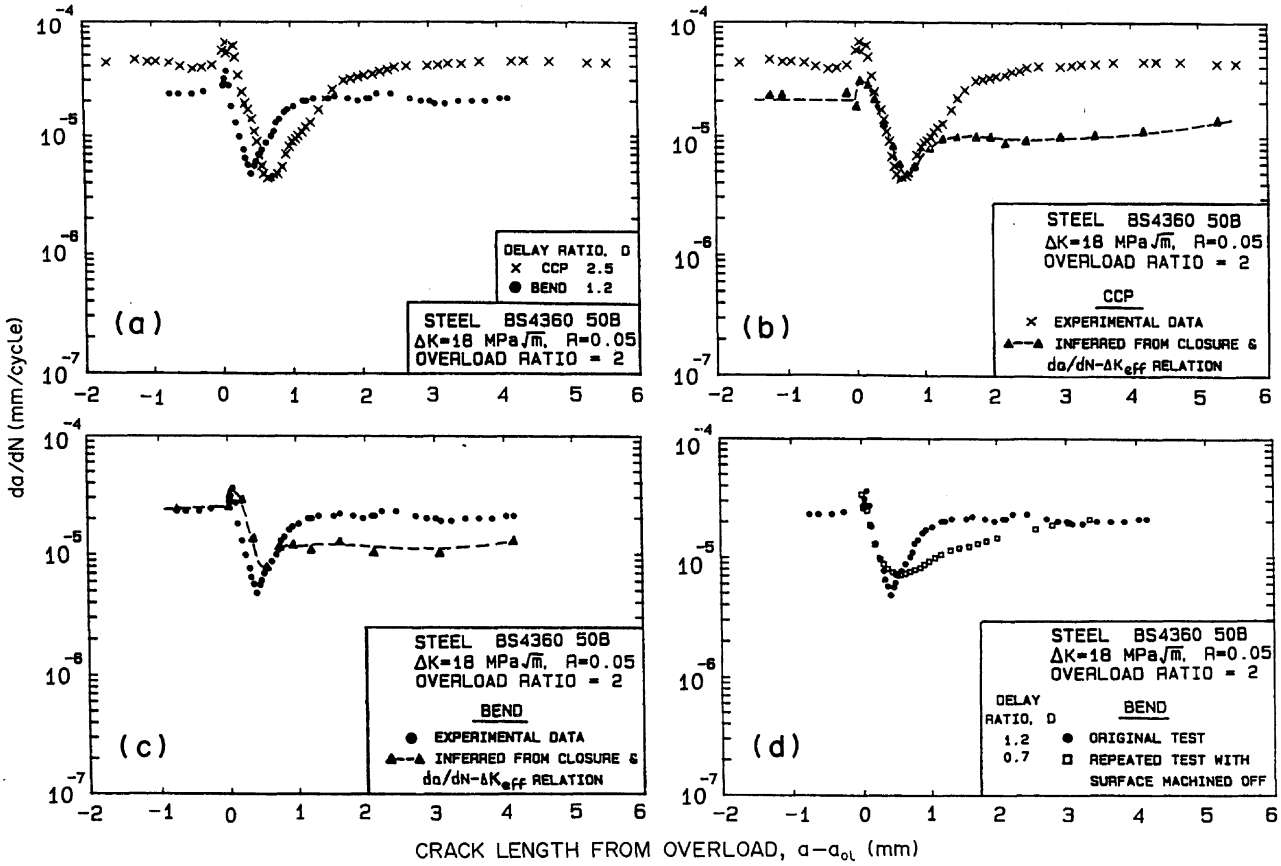

Fig. 5. Measured crack growth rates following a single overload in steel BS 4360 50B. (a) $K_{ol}/\sigma_y\sqrt{W} = 0.39$ (CCP), 0.48 (Bend). (b) Measured and inferred growth rates (CCP). (c) Measured and inferred growth rates (Bend). (d) Showing effect of surface maching immediately after the overload.

In the aluminium alloy the closed crack increment appears to be below the sensitivity of the closure instrumentation. For example, in the Bend specimen, Fig. 4(d), no change in closure response was detected following overload. This was also the case for tests in the aluminium alloy at $R = 0.5$; no closure transient was detected.

The closure transients may be compared directly with the FEM predictions of Fig. 2. The crack growth increment from the overload is in this case normalised by $(K_{ol}/\sigma_y)^2$. Figure 6(a, b) show P_{op}/P_{max} against normalised crack growth increment for the aluminium and steel tests respectively at low R in which the overload ratio was 2. Values of $K_{ol}/\sigma_y\sqrt{W}$ and T_{ol}/σ_y are shown on the figures for comparison with the FEM value. In all cases the closure data shows the expected trends, with the CCP values lying above those for Bend specimens. The numerical agreement is reasonable, with increasing disparity at larger growth increments due to discontinuous closure. The difficulty in measuring the closure transient in the aluminium alloy is again evident. Datapoints separated by the same physical crack growth increment are much further apart on the normalised axes in the case of aluminium than in the steel.

We conclude that specimen geometry influences the overload transient, with more severe retardation in the CCP than the Bend geometry. This agrees with the findings of Tanaka *et al.* [10] using HT80 steel and A5083 aluminium alloy in the same geometries. Crack closure was difficult to measure when the closed crack increment was small, particularly in the aluminium alloy. At high R (= 0.5) no closure transient could be detected though crack growth was retarded. Turner *et al.* [11] found the same behaviour, and in the summary to the symposium in which their work was presented [12] it was suggested that the sensitivity of their closure instrumentation may have been

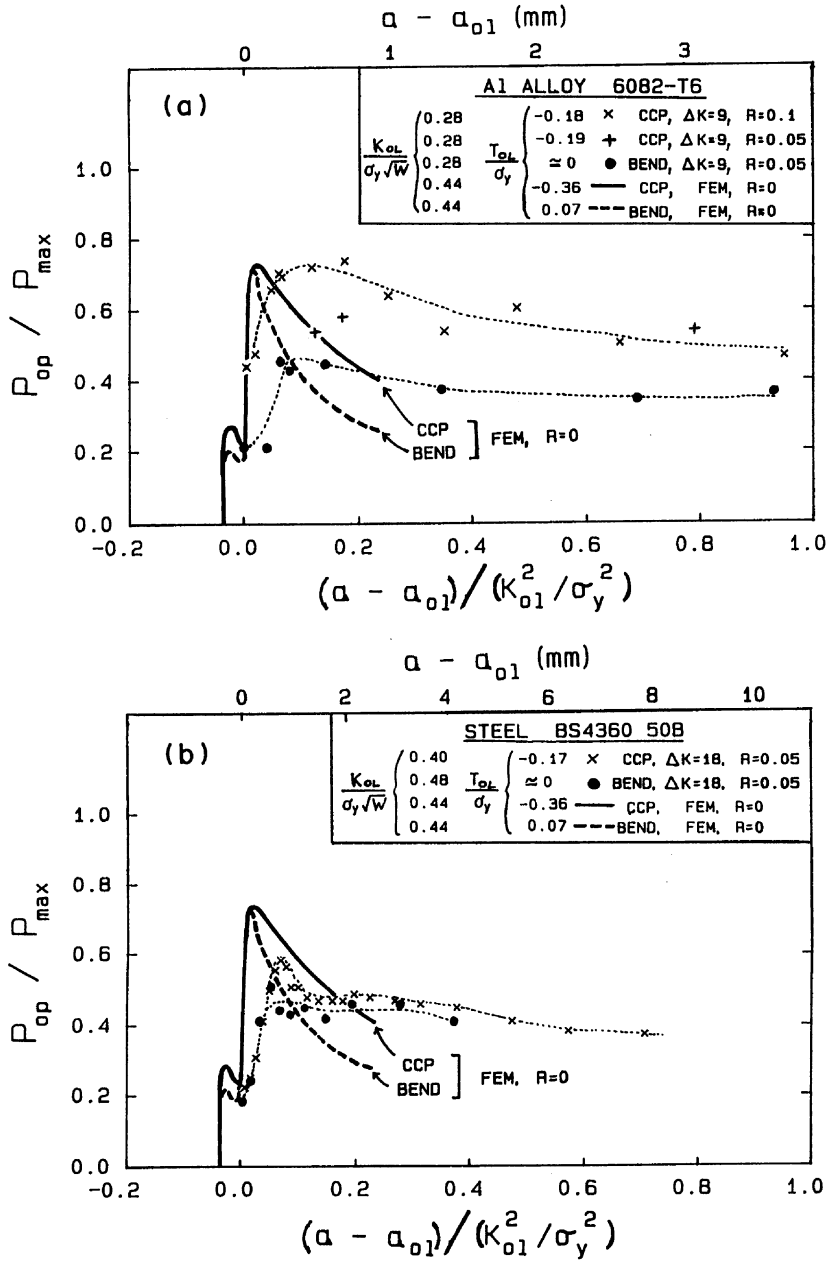

Fig. 6. Comparison of measured crack opening response following an overload with those predicted by FEM. In all cases, the overload cycle is of range twice the baseline loading. (a) Aluminium alloy 6082-T6. (b) Steel BS 4360 50B.

inadequate. It would be useful to obtain an FEM prediction of the macroscopic load–displacement relation for points straddling the crack for cases in which closure could not be detected experimentally.

Discontinuous closure was observed in all tests at $R = 0.05$, in agreement with the FEM prediction, Fig. 3(b).

SPECIMEN MACHINED AFTER OVERLOAD

It has been argued that the retardation following an overload is entirely due to near surface yielding, since this is more extensive than in the bulk of the specimen. To investigate this, a steel

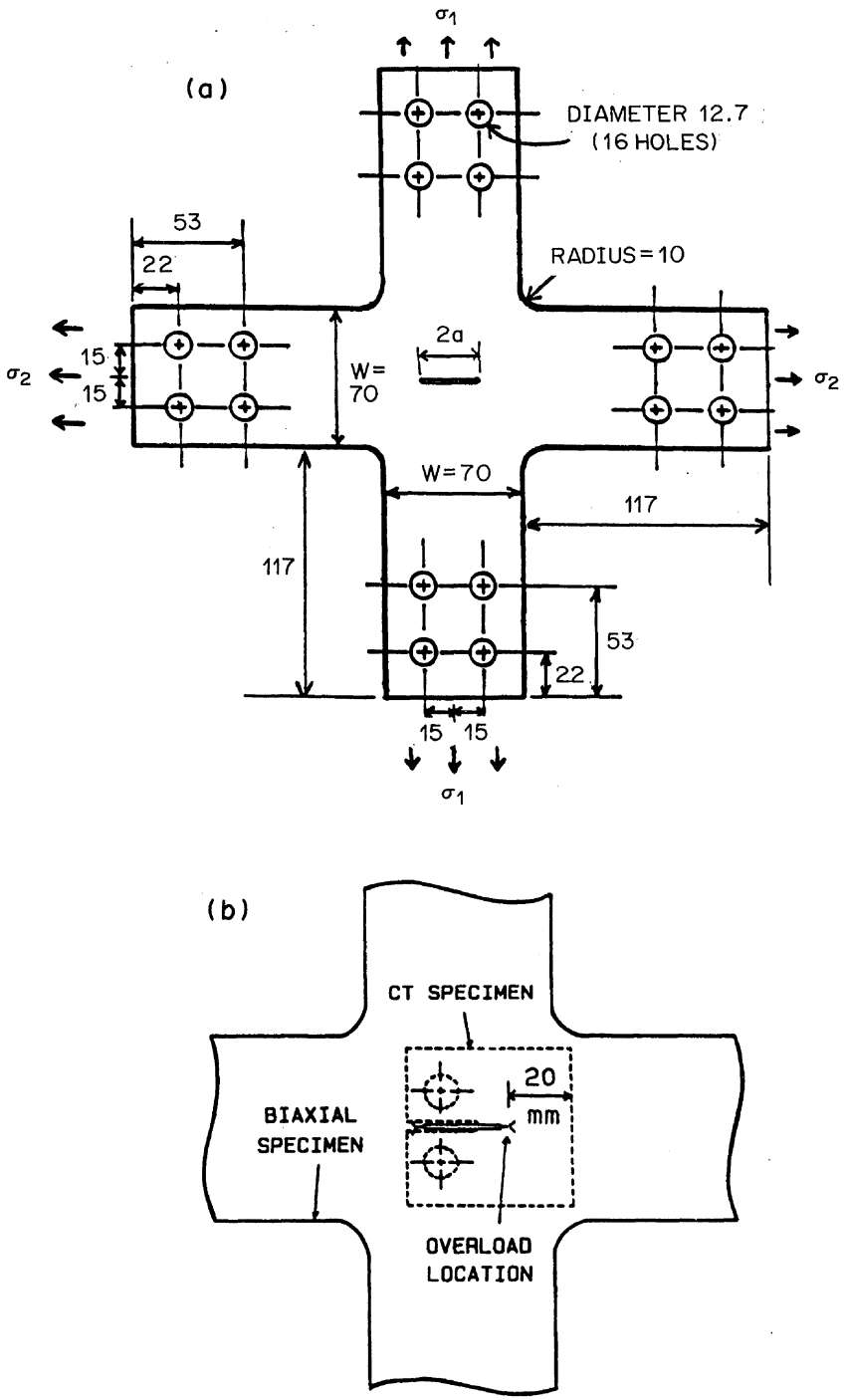

Fig. 7. Biaxial test specimen geometry. (a) Full specimen; dimensions in mm. (b) Location of CT specimen machined out following biaxial overload.

Bend specimen was overloaded and the side faces machined off to a depth of 2 mm. The machined depth was chosen to equal the calculated surface plastic zone size, r_{ps}. Fleck [9] gives this as $r_{ps} = (1/2\pi)\,(K_{ol}/\sigma_y)^2$. After machining, fatigue loading was resumed at the baseline ΔK with suitably reduced loads.

Results with further test details are shown in Fig. 5(d). The crack growth rate transient in a duplicate test in which no machining was carried out is included in the figure. The retardation is less severe in the thinned specimen but persisted for a larger growth increment. While it is believed

that corrosion of the crack faces has occurred, due to penetration of machining fluid, it is clear that the retardation transient has not been eliminated by removing the surface overload plastic zones.

BIAXIAL TESTS

Two biaxial tests were performed using the same K_{ol} but different T-stress values. Biaxial specimens were machined from 12 mm thick BS4360 50B steel plate. Figure 7(a) shows the symmetrical cruciform shape of the specimen. It was possible to use a small corner radius as the specimen received only a single biaxial cycle. With many cycles of load fatigue cracking from this radius is likely.

The test procedure was as follows. An initial notch was cut, and a 1 mm pre-crack was grown from each tip of the slot using uniaxial tensile loading, σ_1, applied perpendicular to the crack [see Fig. 7(a)]. Pre-cracking was carried out at $\Delta K \simeq 15\ \text{MPa}\sqrt{\text{m}}$ and $R = 0.05$, based on the CCP calibration (neglecting the side arms of the specimen). The constraint of the side arms resulted in a lower ΔK, which necessitated a large number of cycles to develop the pre-crack.

A K-calibration and stress analysis of the biaxial specimen was carried out by Dr Paul Tan of NASA Langley, using the boundary force method [13]. The results are presented in Fig. 8.

Biaxial overloads were applied to two specimens such that K_{ol} was the same in each case, while the T-stress was varied by a factor of 3 from $-0.19\ \sigma_y$ to $-0.58\ \sigma_y$. The value of K_{ol} was equivalent to an overload ratio of 2 for a baseline loading of $\Delta K = 15\ \text{MPa}\sqrt{\text{m}}$ and $R = 0.05$. In the first test a tensile transverse load was applied to reduce the compressive stress induced by the specimen geometry due to the normal load. In the second test a compressive transverse load was applied to increase the magnitude of the T-stress. The loads which could be applied were limited by specimen yielding.

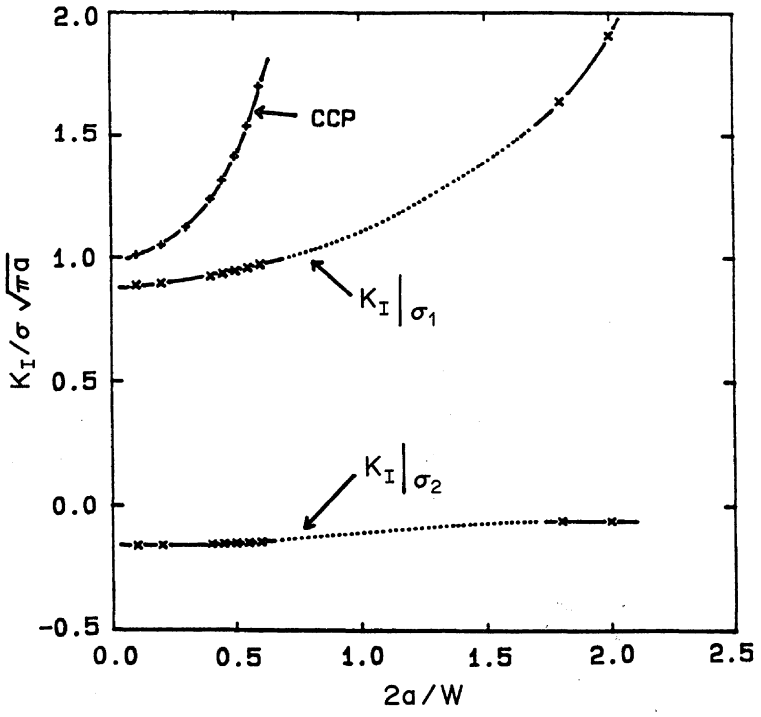

Fig. 8. The K-calibration of the biaxial test specimen. The values of $K_I/\sigma\sqrt{\pi a}$ due to normal (σ_1) and transverse (σ_2) stresses were evaluated using the boundary force method; the analytical calibration for the CCP geometry is also shown.

Following the overload, a compact tension specimen was machined from the biaxial specimen as shown in Fig. 7(b). Baseline loading at $\Delta K = 15\ \text{MPa}\sqrt{\text{m}}$ and $R = 0.05$ was resumed as in the uniaxial tests, using a back face strain gauge to monitor crack closure. It was assumed that the transient closure and crack growth depended on the residual effects of the overload. The compact tension geometry was particularly convenient for measuring crack growth through the overload plastic zone.

The crack growth rates following the overload for the two biaxial tests are shown against the crack growth increment in Fig. 9(a). The value of delay ratio, calculated as before, is also shown. The second test showed a lower minimum growth rate and slightly higher value of D. This is due to the larger plastic zone in this test which is a consequence of the higher magnitude of the compressive T-stress. The influence of T-stress is consistent with the FEM results and the uniaxial tests: the retardation is more severe for the larger negative value of T_{ol}/σ_y.

Figures 9(b, c) show the crack growth transients for each test, with the values inferred from the measured closure and the characteristic da/dN vs ΔK_{eff} relation. As in the uniaxial tests, discontinuous closure occurs as the crack growth rate recovers to the baseline level. The disparity between measured and inferred growth rates is more marked in the second test in which the overload plastic zone was larger.

SIMPLE MODEL OF OVERLOAD RETARDATION

A simple model is now developed in order to predict retardation following an overload on the basis of plasticity-induced crack closure. From an assumed distribution of residual stress induced by the overload, a transient K_{op} vs crack extension Δa response is calculated and hence the retardation behaviour. In more detail, the model consists of the following steps:

1. Following Stouffer and Williams [14], the crack tip stress distribution found by Rice [15] for mode III loading is used to estimate the stress component σ_{yy} normal to the cracking plane as a function of distance x ahead of the crack tip

$$\sigma_{yy}\epsilon_{yy} = \frac{K^2}{\pi(1+n)Ex}. \tag{2}$$

   Here ϵ_{yy} is the local true strain component related to σ_{yy} via the constitutive law for power law hardening

$$\epsilon_{yy} = \frac{\sigma_{yy}}{E} + \left[\frac{\sigma_{yy}}{A}\right]^{1/n} \tag{3}$$

   E is Young's modulus, n is the strain hardening exponent and A is a material constant.
2. Equation (2) predicts unbounded stresses at the crack tip. Accordingly the stress field at $K = K_{ol}$ is calculated by offsetting the stress field by a small distance x_0

$$\sigma_{yy}\epsilon_{yy} = \frac{K_{ol}^2}{\pi(1+n)E(x+x_0)} \tag{4}$$

   such that the stress σ_{yy} at $x = 0$ equals the tensile strength of the material.
3. The residual stress field induced by the overload σ_{res} is found by subtracting the stress field, $\Delta\sigma_{yy}$ due to unloading from K_{ol} to K_{min}, from the stress field at overload, $K = K_{ol}$. It is assumed that $\Delta\sigma_{yy}$ is given by

$$\Delta\sigma_{yy}\Delta\epsilon_{yy} = \frac{(K_{ol}-K_{min})^2}{\pi(1+n)2E(x+x_0)} \tag{5}$$

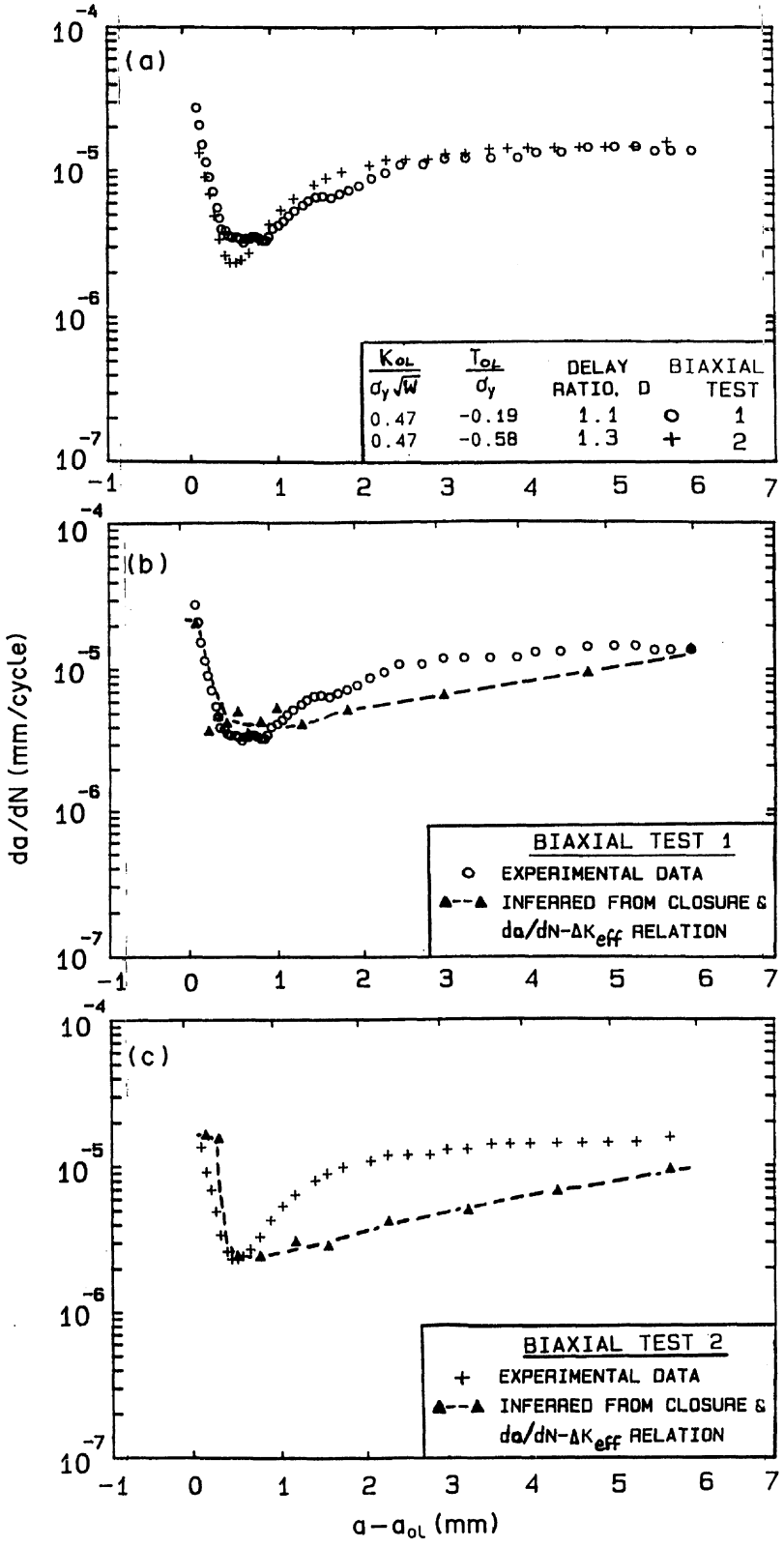

Fig. 9. Biaxial fatigue crack growth rates for the steel BS 4360 50B when $\Delta K = 15\,\text{MPa}\sqrt{\text{m}}$, $R = 0.05$, overload ratio = 2. (a) Crack growth rates following biaxial overloads in two tests. (b) Measured and inferred crack growth rate, test 1. (c) Measured and inferred crack growth rate, test 2.

where $\Delta\epsilon_{yy}$ is related to $\Delta\sigma_{yy}$ via

$$\frac{\Delta\epsilon_{yy}}{2} = \frac{\Delta\sigma_{yy}}{2E} + \left[\frac{\Delta\sigma_{yy}}{2A}\right]^{1/n}. \tag{6}$$

4. If crack advance into the overload region is simulated using a fine sawcut, while holding the load constant at the minimum load following the overload, P_{min}, then the residual compressive stresses hold the crack shut. Hence it is argued that the stress field σ_{res} is the origin of K_{op} during crack growth through the overload plastic zone. Assume that the crack has advanced from the crack length at overload, a_{ol}, to a greater length, a. The K_{op} transient is assumed to take the form

$$K_{op}(a) = K_{min} + \int_0^{a-a_{ol}} \frac{1}{\sqrt{2\pi}} \sigma_{res}(x)(a - a_{ol} - x)^{-1/2}\, dx \tag{7}$$

where K_{min} is the minimum stress intensity of baseline fatigue loading and $[2\pi(a - a_{ol} - x)]^{-1/2}$ is the Green's function for a point load a distance $(a - a_{ol} - x)$ from the tip of a semi-infinite crack in an infinite plate. Equation (7) predicts that K_{op} increases with crack extension to a maximum value before decaying again to K_{min}. When K_{op} falls to the value associated with constant amplitude baseline loading the baseline value is used rather than equation (7).

Predictions of the model

The predictions of this model are compared in Fig. 10 with experimental results described previously for BS4360 50B steel [7]. Test details are included in the figure. In order to examine the sensitivity of predicted crack growth rates with respect to a change of residual stress distribution, predictions are included for the case where the factor of π in equations (2) and (5), shown by the full line in Fig. 10, is replaced by $\pi/2$, shown by the dashed line in Fig. 10.

It is apparent from Fig. 10 that the predicted crack growth rate is very sensitive to the magnitude of the residual stress distribution. Assuming that a factor of π is used in equations (2) and (5), the model is able to predict the retardation transient to within a factor of about 3 for the thin specimens [see Fig. 10(a)–(c)]. It is less accurate for the case of the 24 mm thick specimens [Fig. 10(d)] where plane strain conditions prevail along most of the crack front. In this case, the predicted growth rates are up to 5 times slower than the measured growth rates and the model predicts retarded growth over a crack growth increment of about 3 times the observed value. This is consistent with the fact that the overload plastic zone size is much smaller under plane strain conditions than under plane stress conditions.

The model above is crude but has support on the following physical and theoretical grounds:

1. Allison [16] has observed with the X-ray method that the residual stress field induced by an overload is not relaxed significantly by subsequent fatigue crack growth.
2. The model shows explicitly the manner in which residual stresses induced by the overload lead to increased closure values.
3. The assumed residual stress field σ_{res} resembles the Hutchinson–Rice–Rosengren field near the crack tip, and decays to the required elastic K-field far from the crack tip.
4. The sign of σ_{res} changes from compression to tension with increasing distance ahead of the crack tip from the overload position. Discontinuous closure is predicted in such a field.

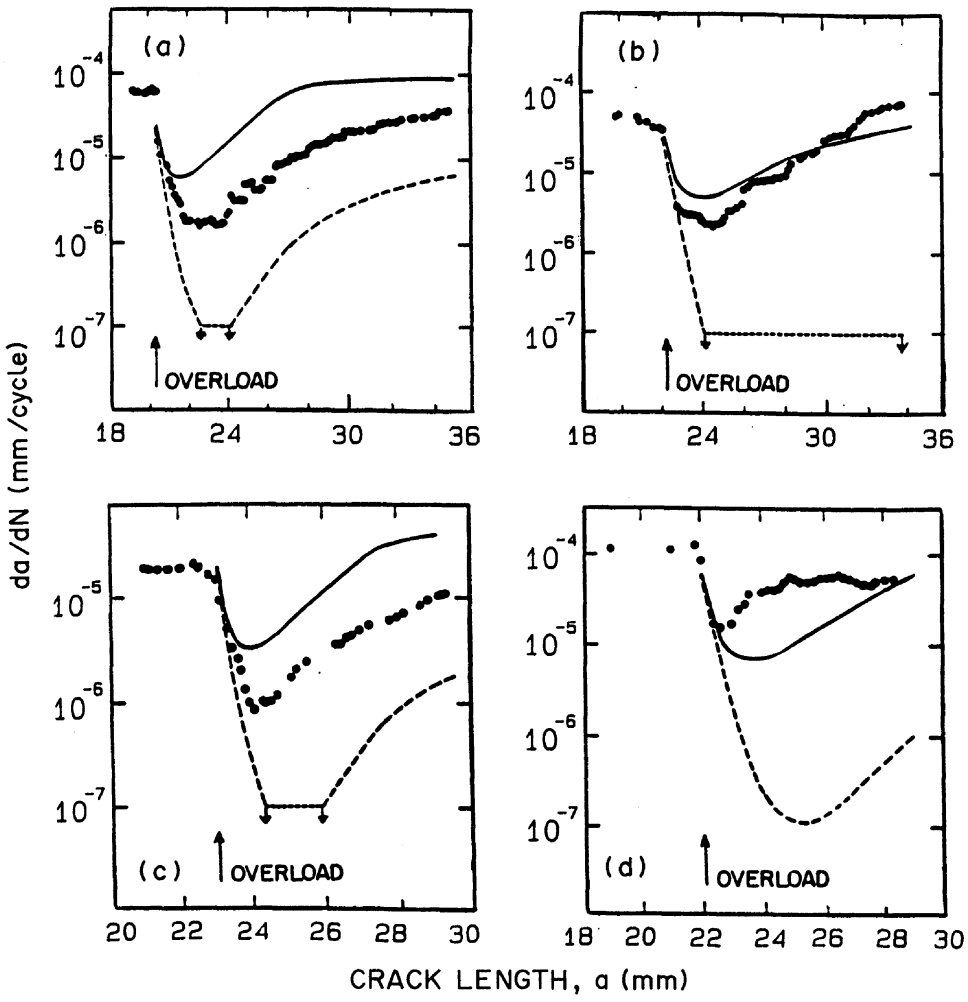

Fig. 10. Comparison of measured crack growth rates following an overload with those predicted by the simple model, for steel BS 4360 50B. In all cases, the overload cycle is of range twice the baseline loading. Baseline loading conditions for 3 mm thick specimens (plane stress): (a) $\Delta K = 25$ MPa$\sqrt{\text{m}}$, $R = 0.05$; (b) $\Delta K = 25$ MPa$\sqrt{\text{m}}$, $R = 0.3$; (c) $\Delta K = 20$ MPa$\sqrt{\text{m}}$, $R = 0.05$, and for 24 mm thick specimen (plane strain); (d) $\Delta K = 25$ MPa$\sqrt{\text{m}}$, $R = 0.05$.

5. The finite element results, Fig. 2, suggest that retardation is not influenced by specimen geometry under plane stress conditions, and the simple model suffices. Under plane strain conditions, retardation is dependent upon specimen geometry via the T-stress, and a more complex retardation model is required.

CONCLUSIONS

Experimental and theoretical support is given for the hypothesis that plasticity-induced crack closure is one of the main causes of overload retardation, under both plane stress and plane strain conditions. Finite element results suggest that specimen geometry has a significant influence on crack growth delay, via the T-stress, when the specimen is sufficiently thick for plane strain conditions to prevail near the crack tip. Biaxial tests confirmed the influence of the T-stress. Discontinuous closure occurs after overloads in aluminium alloy and steel, as predicted by FEM analysis. A simple mechanics model has been developed which demonstrates the relationship between overload-induced residual stresses ahead of the crack tip and plasticity-induced crack closure.

Acknowledgements —The authors wish to acknowledge the support of Dr J. C. Newman Jr and the NASA Langley Research Centre through NASA Grant NAGW-1014, and to thank Dr P. Tan for providing an analysis of the biaxial specimen.

REFERENCES

1. J. C. Newman Jr (1976) A finite element analysis of fatigue crack closure, *Mechanics of Crack Growth, ASTM STP 590*, pp. 281–301. ASTM, Philadelphia, Pa.
2. N. A. Fleck (1986) Finite element analysis of plasticity-induced crack closure under plane strain conditions. *Engng Fract. Mech.* **25,** 441–449.
3. N. A. Fleck and J. C. Newman Jr (1988) Analysis of crack closure under plane strain conditions. *Mechanics of Fatigue Crack Closure* (edited by J. C. Newman and W. Elber), *ASTM STP 982*, pp. 319–341. ASTM, Philadelphia, Pa.
4. J. C. Nagtegaal, D. M. Parks and J. R. Rice (1974) On numerically accurate finite element solutions in the fully plastic range. *Comput. Meth. Appl. Mech. Engng* **4,** 153–177.
5. S. G. Larsson and A. J. Carlsson (1973) Influence of non-singular stress terms and specimen geometry on small-scale yielding at crack tip in elastic-plastics materials. *J. Mech. Phys. Solids* **2,** 263–277.
6. N. A. Fleck, I. F. C. Smith and R. A. Smith (1983) Closure behaviour of surface cracks. *Fatigue Engng Mater. Struct.* **6,** 225–239.
7. N. A. Fleck (1988) Influence of stress state on crack growth retardation. *Basic Questions in Fatigue: Volume I* (Edited by J. T. Fong and R. J. Fields), *ASTM STP 924*, pp. 157–183. ASTM, Philadelphia, Pa.
8. N. A. Fleck (1982) The use of compliance and electrical resistance techniques to characterise fatigue crack closure. Cambridge Univ. Engng Dept, Rep. CUED/C-MATS/TR89.
9. N. A. Fleck (1984) An investigation of fatigue crack closure. Cambridge Univ. Engng Dept, Rep CUED/C-MATS/TR104.
10. K. Tanaka, S. Matsuoka, V. Schmidt and M. Kuna (1981) Influence of specimen geometry on delayed retardation phenomena of fatigue crack growth in HT80 steel and A5083 aluminium alloy. *Proc. ICF5*, Vol. 4, pp. 1789–1798.
11. C. C. Turner, C. D. Carman and B. M. Hillberry (1988) Fatigue crack closure behaviour at high stress ratios. *Mechanics of Fatigue Crack Closure*, (Edited by J. C. Newman Jr and W. Elber), *ASTM STP 982*, pp. 528–535. ASTM, Philadelphia, Pa.
12. J. C. Newman Jr and W. Elber (1988) *Summary, Mechanics of Fatigue Crack Closure* (Edited by J. C. Newman Jr and W. Elber), *ASTM STP 982*, p. 638. ASTM, Philadelphia, Pa.
13. P. W. Tan, I. S. Raju and J. C. Newman Jr (1986) Boundary force method for analysing two-dimensional cracked bodies. NASA Tech. Memorandum 87725, NASA Langley.
14. D. C. Stouffer and J. F. Williams (1979) A model for fatigue crack growth with a variable stress intensity factor. *Engng Fract. Mech.* **11,** 525–536.
15. J. R. Rice (1967) Stress due to a sharp notch in a work hardening elastic-plastic material loaded in longitudinal shear. *J. appl. Mech.* **34,** 287–298.
16. J. E. Allison (1979) Measurement of crack tip stress distributions by X-ray diffraction. *Fracture Mechanics* (Edited by C. W. Smith), *ASTM STP 677*, pp. 550–562. ASTM, Philadelphia, Pa.